Measuring Atmospheric Neutrinos at the Sudbury Neutrino Observatory

T. J. Sonley*† for the SNO Collaboration

Laboratory for Nuclear Science, Massachusetts Institute of Technology, Cambridge, MA 02139
†*Current Address: Department of Physics, University of Utah, Salt Lake City, UT 84112*

***Abstract*. The Sudbury Neutrino Observatory is a 1 kiloton water Cerenkov detector with the ability to track high energy muons created from cosmic ray showers and atmospheric neutrino interactions. The cosmic ray muon flux at SNO is measured to be 3.31 ± 0.09 x 10^{-10} muons per second per square centimeter, and is confined to zenith angles with $\cos\theta_{\rm zenith}>$ 0.4. For larger zenith angles, muons produced in atmospheric neutrino interactions dominate the flux. Neutrinos from below the horizon will have undergone oscillations, while the neutrinos from above the horizon will not have. This allows for a measurement of the neutrino-induced muon flux where the effect of neutrino oscillations is minimized. The measured zenith angle distribution is consistent with previously measured neutrino oscillation parameters. The measured neutrino flux is 1.22 ± 0.09 times larger than predicted by the Bartol three-dimensional flux model.**

***Keywords*: Atmospheric Neutrino Flux**

I. INTRODUCTION

The Sudbury Neutrino Observatory (SNO) is a large water-cherenkov detector located in Ontario, Canada at a depth of 2 km with a flat overburden. The combination of large depth and flat overburden attenuates almost all cosmic-ray muons entering the detector at zenith angles less than $\cos\theta_{\rm zenith}$= 0.4. Because of this depth, SNO is sensitive to neutrino-induced through-going muons over a large range of zenith angles, including angles above the horizon. Measuring the through-going muon flux as a function of zenith angle for $\cos\theta_{\rm zenith} < 0.4$ provides sensitivity to both the oscillated and un-oscillated portions of the atmospheric neutrino flux. Measuring the muon angular spectrum above this cutoff provides access to the flux of cosmic-ray muons created in the upper atmosphere. This paper summarizes a measurement of the flux of muons traversing the SNO detector described in detail elsewhere [1].

II. THE SUDBURY NEUTRINO OBSERVATORY

The Sudbury Neutrino Observatory is located in the Vale-Inco Creighton mine near the city of Sudbury, Ontario at a depth of 2092 ± 6 meters from the Earth's surface. The total depth to the center of the SNO detector, taking into account air and water filled cavities, is 5890 ± 94 meters water equivalent.

The SNO detector itself includes a 6 m radius acrylic vessel filled with heavy water (D_2O). The acrylic vessel is surrounded by 7.4 kilotonnes of ultra-pure H_2O encased within an approximately barrel-shaped cavity measuring 34 m in height and 22 m in diameter. A 17.8-meter diameter stainless steel geodesic structure surrounds the acrylic vessel. The geodesic is equipped with 9456 20-cm photo-multiplier tubes (PMTs) pointed toward the center of the detector.

Data taking in the SNO experiment is subdivided into three distinct phases: pure D_2O, D_2O + Salt, and D_2O + discrete ^{3}He proportional counters. The phases were designed to provide complementary measurements of the solar neutrino flux, and are described in detail elsewhere [1]. The through-going muon analysis uses all three phases of the experiment. After incorporating numerous calibrations, the reconstruction efficiency and acceptance for through-going muons is found to be equivalent for all phases.

III. SIMULATION

In order to understand the measured neutrino-induced flux, a model of the initial neutrino flux and subsequent propagation is necessary. SNO uses the Bartol group's three-dimensional calculation of the atmospheric neutrino flux [2]. Current estimates of the neutrino flux uncertainties are approximately $\pm 15\%$ and depend strongly on neutrino energy. Because the normalization of the neutrino flux and the energy spectral shape are highly correlated, the fits to the data reported herein assume a fixed neutrino energy spectrum. We also assume that the flux and energy spectra do not change significantly with solar activity. Although variations throughout the solar cycle are expected, the majority of this variation is confined to neutrinos of energy below 10 GeV, so the impact on the fluxes predicted at SNO is expected to be small.

Neutrino interactions in the rock surrounding the detector are simulated by the NUANCE v3 Monte Carlo neutrino event generator [3]. NUANCE includes a comprehensive model of neutrino cross sections applicable across a wide range of neutrino energies. Transport of muons through the rock from neutrino-induced interactions is calculated using the PROPMU muon transport code [4], which is integrated into the NUANCE Monte Carlo framework. Simulation of muon transport in the D_2O and H_2O and subsequent detector response is handled by the SNO Monte Carlo and Analysis (SNOMAN) code. SNOMAN propagates the primary particles and any secondary particles (such as Compton electrons) that are created, models the detection of the optical photons by the PMTs, and simulates the electronics response. The SNOMAN code has been benchmarked against calibration neutron, gamma, and electron data taken during the lifetime of SNO.

In addition to the through-going signal from atmospheric neutrinos, a number of backgrounds which have muon signatures are simulated in the analysis. These include ν_μ interactions inside the H_2O and D_2O volumes of the detector, and ν_e interactions that either have a muon in the final state or are misidentified as a through-going muon. Cosmic-ray muons incident on the detector constitute an additional source of high-energy muons and are treated separately. Transport of such high-energy muons in the rock is performed by the MUSIC muon transport code [5].

IV. Event Selection

The through-going muon fitter uses charge and timing information from each PMT in the detector to find the best fit track. The charge and timing distributions are conditional on the number of expected photoelectrons incident on a given PMT based on a library of simulated tracks. Monte Carlo studies indicate that approximately 87% of all simulated muons with an impact parameter of less than 830 cm reconstruct within 1° of the true track direction. This is confirmed by an external muon tracking detector which ran concurrently with the SNO detector for 94 days of livetime in the third phase of the experiment. An analysis of the 30 events coincident between the two detectors found the resolution of the reconstruction algorithm to be less than 0.6°. Monte Carlo studies also show bias effects on the reconstructed impact parameter to be less than ± 4 cm.

Cuts are applied to the candidate through-going muon events to reject instrumental backgrounds, internal neutrino interactions and badly fit events. These cuts are detailed elsewhere [1] and focus on quantities such as raw charge and timing distributions, deposited energy, and features of the reconstructed Cherenkov cone. The fiducial volume of the detector is defined by a cut on the reconstructed impact parameter of $b_\mu < 830$ cm. If the muon is genuinely through-going (exits the fiducial area of the detector), the total efficiency is 98.0%, based on Monte Carlo studies. The total efficiency is defined as the ratio between the number of through-going cosmic rays that reconstruct with an impact parameter less than 830 cm that pass all cuts versus the number of through-going muon events with a generated impact parameter less than 830 cm.

V. Cosmic-Ray Muon Flux

A total of 76749 muon candidates passing all selection cuts are reconstructed with a zenith angle of $0.4 < \cos\theta_{\rm zenith} < 1$ for the 1229.30-day dataset. The data collected corresponds to an exposure of 2.30×10^{14} cm^2 s. The total measured cosmic-ray muon flux at SNO, after correcting for acceptance, is $(3.31 \pm 0.01\ (\rm stat.) \pm 0.09\ (\rm sys.)) \times 10^{-10}$ μ/s/cm^2, or 62.9 ± 0.2 muons/day passing through a 830-cm radius circular fiducial area.

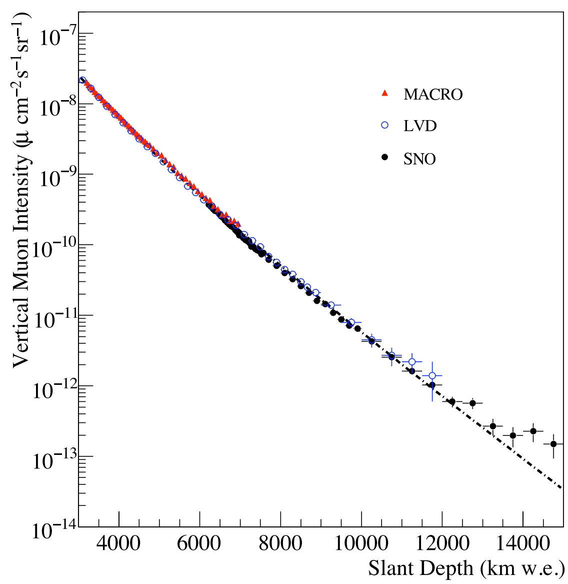

Fig. 1. The flux of cosmic-ray muons that pass all cuts as a function of standard rock depth. SNO data (filled circles) shown with best global fit intensity distribution (dashed line) and data the from the LVD [6] (empty circles) and MACRO [7] (triangles) detectors using Eq. 1. Global fit range extends to 13.5 kilometers water equivalent, beyond which atmospheric neutrino-induced muons start to become a significant fraction of the signal.

The vertical muon intensity as a function of depth can be calculated by binning the above data as a function of slant depth, and can be parameterized by:

$$I_\mu^v(x_{\rm std}) = I_0\ (\frac{x_0}{x_{\rm std}})^\alpha\ e^{-x_{\rm std}/x_0} \qquad (1)$$

where I_0 is an overall normalization constant, and x_0 represents an effective attenuation length for high-energy muons. The remaining free parameter, α, is strongly correlated with the spectral index of the muon flux at the surface of the earth, γ. Results from fits of the vertical muon intensity as a function of depth for various values of these parameters are shown in Table I. We perform fits whereby the parameter α is either fixed to what one would expect from the surface ($\alpha = \gamma - 1 = 1.77$) or allowed to float freely. The cosmic-ray data tends to prefer larger values of α than the expected value of 1.77. A comparison of SNO's muon flux to that measured in the LVD [6] and MACRO [7] is shown in Figure 1. In general, there exists tension between the different data sets. Fits have been performed both with and without allowing the slant depth uncertainty to float within its uncertainty. The fits in both cases are nearly identical, with minimal change ($< 1\sigma$) to the slant depth. The fits presented in Table I are with the slant depth constrained. More information about the fitting

Dataset	I_0 (10^{-6} cm^{-2} s^{-1} sr^{-1})	x_0 (km w.e.)	α	χ^2/dof
SNO only	1.20 ± 0.69	2.32 ± 0.27	5.47 ± 0.38	34.2 / 44
SNO only	2.31 ± 0.32	1.09 ± 0.01	1.77	111.0 / 45
SNO + LVD + MACRO	2.16 ± 0.03	1.14 ± 0.02	1.87 ± 0.06	230.2/134

TABLE I

RESULTS FROM THE SNO FIT TO THE VERTICAL MUON INTENSITY FOR $\cos\theta_{\text{zenith}} > 0.4$ USING EQUATION 1. THE FITS WERE PERFORMED EITHER USING ONLY SNO DATA WITH THE α PARAMETER ALLOWED TO FLOAT, WITH THE α PARAMETER FIXED TO 1.77, OR COMBINED WITH LVD [6] AND MACRO [7] COSMIC RAY DATA. SYMBOLS IN THE TABLE ARE AS DEFINED IN THE TEXT. THE ERRORS REPORTED ARE A COMBINATION OF STATISTICAL AND SYSTEMATIC UNCERTAINTIES ON THE FLUX AND SLANT DEPTH.

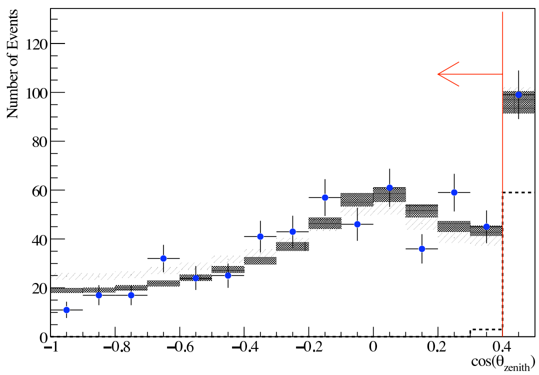

Fig. 2. The distribution of through-going neutrino-induced muons that pass all cuts as a function of zenith angle. Data (crosses) are shown with the best-fit MC spectra of $(\Phi_0, \sin^2 2\theta, \Delta m^2)$ = (1.22 ± 0.10, 1.00, 2.6×10^{-3} eV^2) (solid box) and prediction with no neutrino oscillation and a best fit normalization of $\Phi_0 = 1.09 \pm 0.08$ (hashed box). The background due to cosmic-ray muons is shown in the dashed line. The zenith angle cut is indicated in the figure.

procedure and additional model-independent fits may be found elsewhere [1].

VI. ATMOSPHERIC NEUTRINO RESULTS

To fit for the atmospheric neutrino flux and oscillation parameters, we assume a model for the atmospheric neutrino flux, and fit for a total flux scaling factor. In these fits we use a two-neutrino mixing model:

$$\Phi(L/E_\nu, \theta, \Delta m^2)_\mu = \Phi_0 \cdot [1 - \sin^2 2\theta \cdot \sin^2(\frac{1.27\Delta m^2 L}{E_\nu})] \quad (2)$$

where θ is the neutrino mixing angle, Δm^2 is the square mass difference in eV^2, L is the distance traveled by the neutrino in km, E_ν is the neutrino energy in GeV, and Φ_0 is the overall normalization of the neutrino-induced flux.

Figure 2 shows the zenith angle distribution for neutrino-induced muons. A total of 514 events are recorded with $-1 < \cos\theta_{\text{zenith}} < 0.4$ in the 1229.30 days of livetime in this analysis. For neutrino-induced events near the horizon ($\cos\theta_{\text{zenith}}$ between 0 and 0.4), 201 events are observed. Given the current measurements of the atmospheric oscillation parameters, the neutrino-induced flux is unaffected by oscillations in this region and therefore is a direct measurement of the atmospheric neutrino flux, particularly at high energies. The corresponding neutrino-induced through-going muon flux below the horizon ($\cos\theta_{\text{zenith}} < 0$) and above the horizon ($0 < \cos\theta_{\text{zenith}} < 0.4$) are $2.10 \pm 0.12(\text{stat.}) \pm 0.08(\text{sys.}) \times 10^{-13}$cm^{-2}s^{-1}sr^{-1} and $3.31 \pm 0.23(\text{stat.}) \pm 0.13(\text{sys.}) \times 10^{-13}$cm^{-2}s^{-1}sr^{-1}, respectively.

From the measured zenith angle distribution, we can extract the flux normalization Φ_0 and the neutrino mixing parameters θ and Δm^2 in Equation 2. A maximum likelihood fit is performed to find the best fit points. To account for possible distortions in the zenith angle spectrum, we float the systematic uncertainties summarized in table II using a maximum likelihood pull technique [1]. If all parameters are allowed to float, one finds a flux normalization value of $\Phi_0 = 1.22 \pm 0.10$ and best fit neutrino oscillation parameters of Δm^2 of 2.6×10^{-3} eV^2 and maximal mixing. These results are with respect to the Bartol three-dimensional atmospheric flux model [2] and the cross-section model implemented in NUANCE. The zenith angle spectrum is consistent with previously measured neutrino oscillation parameters. One can improve SNO's sensitivity to the atmospheric flux Φ_0 by including existing constraints on the atmospheric neutrino oscillation parameters from the Super-Kamiokande [8] and MINOS [9] neutrino experiments. The constraint reduces the uncertainty on the overall atmospheric neutrino flux normalization to 1.22 ± 0.09. The 68%, 95% and 99.73% confidence level regions for the parameters as determined by the fits are shown in Figure 3. The scenario of no neutrino oscillations by using SNO-only data is excluded at the 99.8% confidence level.

Systematic Error	**ν_μ-induced muon flux error**	**Cosmic-ray muon flux error**
Detector Model	$\pm 3.7\%$	$\pm 1.1\%$
Cross-Section Model	$\pm 3.1\%$	N/A
Propagation Model	$\pm 2.2\%$	$\pm 2.2\%$
Background Events	$\pm 0.8\%$	$\pm 1\%$
Total Systematic Error	$\pm 4.8\%$	$\pm 2.7\%$
Statistical Error	$+8.5\%$	$\pm 0.4\%$

TABLE II

SUMMARY OF SYSTEMATIC ERRORS FOR THE NEUTRINO-INDUCED AND COSMIC-RAY MUON FLUX MEASUREMENTS.

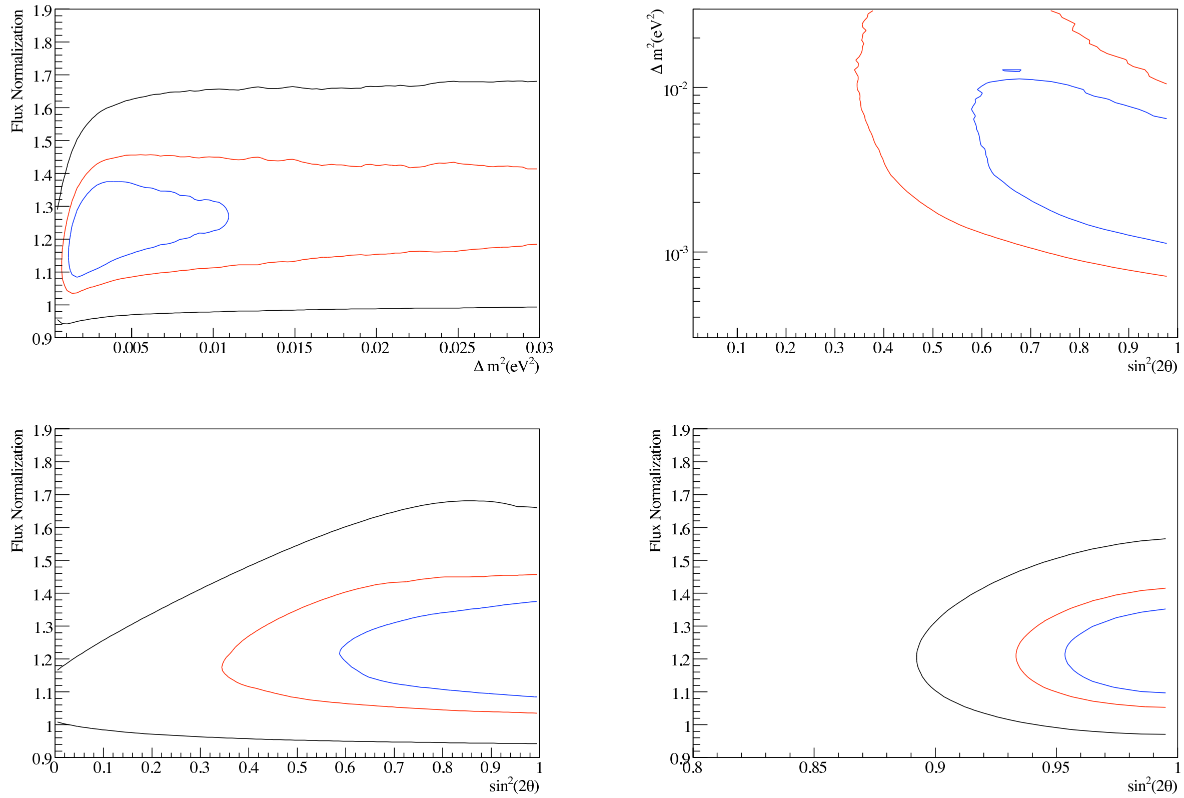

Fig. 3. The 68% (blue), 95% (red), and 99.73% (black) confidence level contours for the ν_μ atmospheric neutrino oscillation parameters based on the muon zenith angle distribution for $\cos\theta_{\rm zenith} < 0.4$. The plots show the SNO-only contours for flux normalization versus mass splitting (top left), SNO-only mass splitting versus mixing angle (top right), SNO-only contours for flux normalization versus mixing angle (bottom left) and the flux normalization versus mixing angle including constraints from the Super-K and MINOS neutrino oscillation experiments (bottom right) [8], [9].

VII. Summary

The Sudbury Neutrino Observatory experiment has measured the through-going muon flux at a depth of 5890 meters water equivalent. We find the total muon cosmic-ray flux at this depth to be $(3.31 \pm 0.01\ (\mathrm{stat.}) \pm 0.09\ (\mathrm{sys.})) \times 10^{-10}$ μ/s/cm^2. We measure the through-going muon flux induced by atmospheric neutrinos. The zenith angle distribution of events rules out the case of no neutrino oscillations at the 3σ level. We measure the overall flux normalization to be 1.22 ± 0.09, which is larger than predicted from the Bartol atmospheric neutrino flux model but consistent within the uncertainties expected from neutrino flux models. This is the first measurement of the neutrino-induced flux above the horizon in the angular regime where neutrino oscillations are not an important effect. The data reported in this paper can be used to help constrain such models in the future.

VIII. Acknowledgments

This research was supported by: Canada: Natural Sciences and Engineering Research Council, Industry Canada, National Research Council, Northern Ontario Heritage Fund, Atomic Energy of Canada, Ltd., Ontario Power Generation, High Performance Computing Virtual Laboratory, Canada Foundation for Innovation; US: Dept. of Energy, National Energy Research Scientific Computing Center; UK: Science and Technology Facilities Council; Portugal: Fundação para a Ciência e a Tecnologia. We thank the SNO technical staff for their strong contributions. We thank Vale Inco for hosting this project.

References

[1] B. Aharmim *et al.* submitted to Phys. Rev. D arXiv:0902.2776v1 [hep-ex]
[2] G. D. Barr *et al.* Phys. Rev. D **70**, 023006 (2004). Flux files can be found at http://www-pnp.physics.ox.ac.uk/~barr/fluxfiles/0408i/index.html for high-energy neutrinos and http://www-pnp.physics.ox.ac.uk/~barr/fluxfiles/0403i/index.html for low-energy neutrinos.
[3] D. Casper, *Nucl. Phys. Proc. Suppl.* 112, 161 (2002).
[4] P. Lipari and T. Stanev, Phys. Rev. D **44**, 3543 (1991).
[5] P. Antonioli, C. Ghetti, E. V. Korolkova, V. A. Kudryavtsev and G. Sartorelli, Astropart. Phys. **7**, 357 (1997).
[6] M. Aglietta *et al.*, Phys. Rev. D58, 092005 (1998).
[7] M. Ambrosio *et al.*, Phys. Rev. D 52(7), 3793 (1995).
[8] Y. Ashie *et al.*, Phys. Rev. D 71, 112005 (2005).
[9] H. Gallagher, J. Phys. Conf. Ser. **136**, 022014 (2008).